

SIMPLIFIED INTEGRATION OF TRIANGULAR NURBS FINITE ELEMENTS

Claudio E. Jouglard^a

^a*Departamento de Ingeniería Civil, Facultad Regional Buenos Aires, Universidad Tecnológica Nacional, Mozart 2300, C1407IVT Buenos Aires, Argentina, claudio.jouglard@frba.utn.edu.ar, <http://www.frba.utn.edu.ar>*

Keywords: NURBS, finite elements, curved domains, simplified integration.

Abstract. In CAD packages, solid objects are represented by a collection of NURBS bounding surfaces and curves. Traditional finite element analysis employs curved elements of limited geometric capability, such as quadratic finite elements whose boundaries are represented by quadratic curves and surfaces that cannot reproduce exactly real life geometries. This complicates the adaptive analysis in curved geometries where there is a need to do a lot of queries to the geometry model to refine the mesh. To overcome this problem, several formulations that consider the exact geometry in the finite element formulation, such as the isogeometric formulation have appeared. In general, these formulations are not simple and requires complex integration rules to obtain the finite element matrices. An alternative representation based on triangular NURBS finite elements, that are triangular elements whose boundaries are NURBS curves is used in this paper. A simplified analytical integration on these elements for planar stress analysis that does not require numerical integration is presented. It and can be easily extended to 3-D nonlinear problems, including contact and plasticity.

1 INTRODUCTION

Nowadays there is a great interest into integration between Computer Aided Design (CAD) and finite element analysis software. Traditionally these areas used different geometric representation of the same domain since their objectives are very distinct. CAD systems are oriented to production and need a very precise description of the geometry and traditional finite element analysis, sometimes, uses a crude approximation of the geometry that is reduced employing a considerable amount of small simple elements (Cottrell et al., 2009).

From an engineering point of view, an accurate description of the geometry is important for adaptive finite element analysis, where the size of the elements is successively reduced until a desired precision is attained, since for this process an exact description of curved boundaries is required to position new nodes and elements. It is also important for the analysis of imperfect structures, like thin shells, where the size of the imperfections (deviations from exact geometry) can have a very negative impact on its stability (Godoy, 1996).

An important step towards reducing the gap between CAD and finite elements was the introduction of the so called Isogeometric Analysis (Hughes et al., 2005) where finite elements based on the same curves and surfaces NURBS (Non Uniform Rational B-Splines) used by CAD systems can reproduce the exact geometry of the model. This simplifies the adaptive refinement process since the geometry information is contained within each finite element.

Isogeometric analysis is not exempt of several problems like trimmed geometries (Marussig and Hughes, 2017) where the intersection of surfaces is not properly approximated by CAD systems leading to the appearance of gaps between intersecting surfaces that invalidate finite element analysis. Isogeometric analysis also uses the same NURBS functions to describe the field of variables and this leads to complicated finite element matrices that need special numerical integration rules (Adam et al., 2015a), (Adam et al., 2015b), (Fahrendorf et al., 2018). Another problem is that solids in CAD are generally modeled only by the surfaces that enclose its volume, so there is a need to construct a volumetric finite element mesh to fill the volume (Cottrell et al., 2007).

An alternative approach is to enrich the classical finite element shape functions with NURBS to exactly reproduce the boundary. A representative method of this class is the NEFEM (NURBS Enriched Finite Element Method) (Sevilla et al., 2008) where the elements only have curved sides and faces at the boundary. There are many variants of this approach (George and Borouchaki, 2012), (Jaxon and Qian, 2014), (Engvall and Evans, 2016), (Xia and Qian, 2017) but all have in common a local representation of the geometry by means of Bezier or rational Bezier triangular functions (Farin, 1986).

In general, the description of the geometry needs more complicated shape functions than the usual low order polynomials used to describe the field of variables. But there is no reason to use the same shape functions for both. Even with low order elements, the desired precision can be achieved by adaptive refinement (Zienkiewicz et al., 2013).

The use of different shape functions to describe the geometry and the variables field is proposed in this paper. The only condition is that in the limit of the adaptive refinement process the geometry of the element converges to a regular shaped finite element with straight sides. In this manner, any classical, hybrid or mixed finite element formulation (Zienkiewicz et al., 2013) independently of the geometry of the finite element can be applied.

To illustrate the proposal, cubic rational Bezier functions to describe the geometry of a triangular finite element will be employed, but only linear polynomial shape functions will be used to describe the field of variables. This, obviously, leads to complicated integrals on curved domains but, to ensure convergence, exact values of these integrals in the limit, when the shape of the element tends to be regular, are only needed. Based on these criteria, a simplified

integration methodology that does not use numerical rules (quadrature free) and recovers the exact values of the integrals in the limit will be presented.

2 BÉZIER REPRESENTATION OF NURBS CURVES AND SURFACES

NURBS curves and surfaces are very popular in CAD systems because they can model not only free form curves but also all the family of conics curves and surfaces, like circles (Piegl and Tiller, 1997).

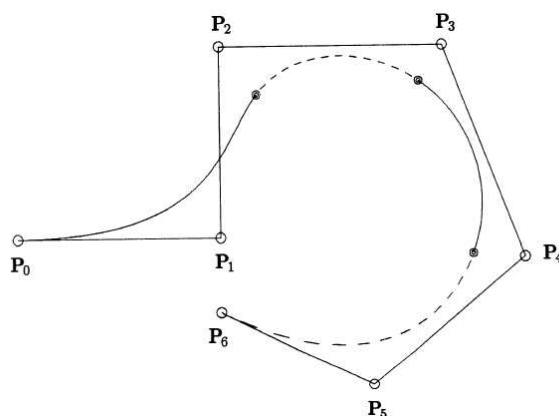


Figure 1: NURBS curve and its control polygon and knots

A NURBS curve is defined by a control polygon with control points \mathbf{P}_i . Geometrically the NURBS curve is formed by several segments with a high degree of continuity between segments. The union of segments occurs at the *knots* of the NURBS curve which are shown on Figure 1.

2.1 Bézier representation of NURBS curves

A Bézier representation of a NURBS curve is a curve segment defined by a control polygon with control points \mathbf{P}_i and their associated weights w_i , where the initial and final points coincide with consecutive knots of the NURBS curve (Farin, 2002) (see Figure 2).

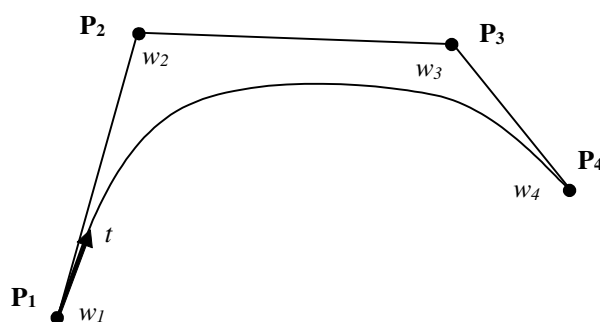


Figure 2: Bézier representation of a NURBS segment.

The rational Bézier curves of degree n are defined parametrically in an interval $[0,1]$ of t as

$$\mathbf{c}(t) = \begin{cases} x(t) \\ y(t) \end{cases} = \frac{\sum_{i=0}^n B_{i,n}(t)w_i\mathbf{P}_i}{\sum_{i=0}^n B_{i,n}(t)w_i} \quad (1)$$

Where functions $B_{i,n}(t)$ are the *Bernstein* polynomials of degree n defined as

$$B_{i,n}(t) = \binom{n}{i} t^i (1-t)^{n-i} \quad (2)$$

The binomial coefficients are

$$\binom{n}{i} = \frac{n!}{i!(n-i)!} \quad (3)$$

In the case of a planar curve the control polygon is contained in the plane of the curve and the control points have two coordinates

$$\mathbf{P}_i = \begin{Bmatrix} x_i \\ y_i \end{Bmatrix} \quad (4)$$

In general, the control points of the Bézier representation are different from the control points of the NURBS curve, but the segments are geometrically identical.

Also, the Bernstein polynomials can be written using barycentric coordinates ξ_1, ξ_2 as

$$B_{i,n}(\xi_1, \xi_2) = \binom{n}{i} \xi_1^i \xi_2^{n-i} \quad (5)$$

Where ξ_1, ξ_2 are the barycentric coordinates in one dimension

$$\begin{aligned} \xi_1 &= t \\ \xi_2 &= 1-t \end{aligned} \quad (6)$$

The barycentric coordinates specify the location of a point of a simplex (a line, a triangle, tetrahedron, etc.) as the center of mass of unequal masses ξ_1, ξ_2 placed at its vertices. Barycentric coordinates are not independent since they are related by

$$\xi_1 + \xi_2 = 1 \quad (7)$$

The barycentric coordinates have other properties that simplify the derivation and integration of functions of these variables over simplices (generalization of a triangle to arbitrary dimensions).

2.2 The rational Bézier triangle

A rational Bézier triangle has NURBS sides which have been reparametrized as Bézier curves. A reference triangle of straight sides with the same vertices of the curved triangle is defined to describe the geometry (see Figure 3).

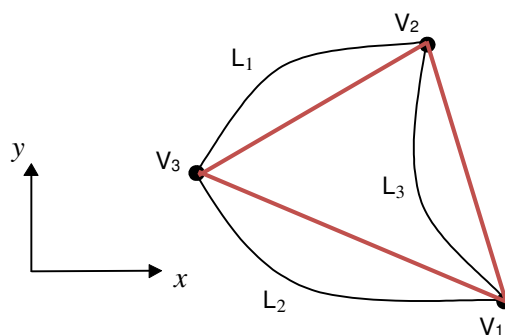


Figure 3: Definition of reference triangle for an element with NURBS boundary

To represent a rational Bézier triangle is necessary to extent the definition of Bernstein polynomials to two dimensions using barycentric coordinates in a triangle (Farin, 2002). The barycentric coordinates for a triangle are the usual area coordinates ξ_1, ξ_2, ξ_3 , (Cook et al., 2001) defined on a reference triangle (see Figure 4).

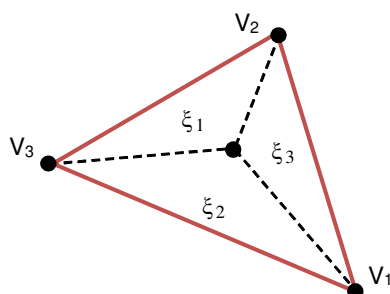


Figure 4: Area coordinates on reference triangle

Any point on the reference triangle can be identified by a unique combination of its barycentric coordinates. As in the previous case, barycentric coordinates are not independent since they are related by

$$\xi_1 + \xi_2 + \xi_3 = 1 \tag{8}$$

Using barycentric coordinates simplifies the definition of interpolation functions on the reference triangle. In particular, Bernstein polynomials of degree n on the triangle are (Farin, 2002)

$$B_{ijk}^n(\xi_1, \xi_2, \xi_3) = \binom{n}{i, j, k} \xi_1^i \xi_2^j \xi_3^k \quad i + j + k = n \tag{9}$$

Where the trinomial coefficients are

$$\binom{n}{i, j, k} = \frac{n!}{i!j!k!} = \frac{n!}{i!j!(n-i-j)!} \tag{10}$$

For example, for $n = 3$ the Bernstein functions are

$$\begin{aligned} B_{300}^3 &= \xi_1^3 & B_{210}^3 &= 3\xi_1^2\xi_2 & B_{120}^3 &= 3\xi_1\xi_2^2 & B_{030}^3 &= \xi_2^3 \\ B_{012}^3 &= 3\xi_2\xi_3^2 & B_{021}^3 &= 3\xi_2^2\xi_3 & B_{102}^3 &= 3\xi_1\xi_3^2 & B_{201}^3 &= 3\xi_1^2\xi_3 \\ B_{003}^3 &= \xi_3^3 & B_{111}^3 &= 6\xi_1\xi_2\xi_3 \end{aligned} \tag{11}$$

Then, we can define a mapping surface $\mathbf{x}(\xi_1, \xi_2, \xi_3)$ of degree n between each point ξ_1, ξ_2, ξ_3 of the reference triangle and a point x, y of the curved triangle by means of $(n+2)(n+1)/2$ control points \mathbf{P}_{ijk} , each one associated to a Bernstein functions on the triangle as

$$\mathbf{x}(\xi_1, \xi_2, \xi_3) = \left\{ \begin{aligned} x(\xi_1, \xi_2, \xi_3) \\ y(\xi_1, \xi_2, \xi_3) \end{aligned} \right\} = \frac{\sum_{i+j+k=n} B_{ijk}^n(\xi_1, \xi_2, \xi_3) w_{ijk} \mathbf{P}_{ijk}}{\sum_{i+j+k=n} B_{ijk}^n(\xi_1, \xi_2, \xi_3) w_{ijk}} \tag{12}$$

For example, for the cubic triangle the control points are located at vertices, thirds of the sides and the centroid of the reference triangle (Figure 5).

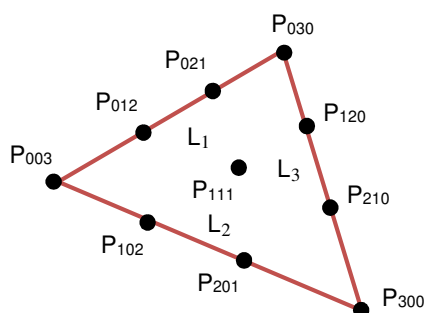


Figure 5: Control points on a cubic Bézier triangle

Bernstein functions for the cubic triangle and the control points can be seen on Figure 6.

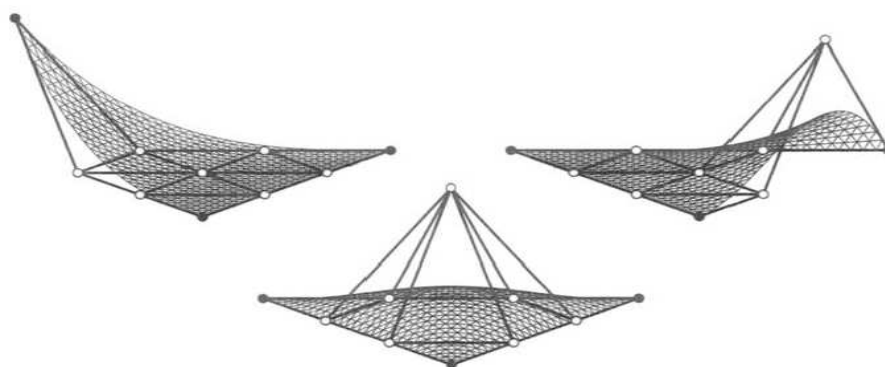


Figure 6: Bernstein functions for the cubic triangle (Farin, 2002)

Defining the shape functions M_{ijk}^n associated to each control point \mathbf{P}_{ijk} then the mapping (12) can be written as

$$\mathbf{x}(\xi_1, \xi_2, \xi_3) = \begin{Bmatrix} x(\xi_1, \xi_2, \xi_3) \\ y(\xi_1, \xi_2, \xi_3) \end{Bmatrix} = \sum_{i+j+k=n} M_{ijk}^n(\xi_1, \xi_2, \xi_3) \mathbf{P}_{ijk} \tag{13}$$

Where

$$M_{ijk}^n(\xi_1, \xi_2, \xi_3) = \frac{B_{ijk}^n(\xi_1, \xi_2, \xi_3)w_{ijk}}{\sum_{i+j+k=n} B_{ijk}^n(\xi_1, \xi_2, \xi_3)w_{ijk}} \tag{14}$$

Note that with an appropriate choice of weights and location of control points it is possible to represent any quadratic or conic curve (like a circle sector) on the boundary (Piegl and Tiller, 1997).

Then, rational Bézier triangles to mesh a planar region whose boundaries are NURBS curves can be used. A planar domain whose boundaries are NURBS curves can be seen in Figure 7.a, the dots on the boundary curves are the knots of the NURBS (Piegl and Tiller, 1997). A NURBS segment can be reparametrized between knots by an equivalent Bézier curve. A discretization with Bézier triangles (Farin, 2002),(Jouglard et al., 2012) is presented in Figure 7.b.

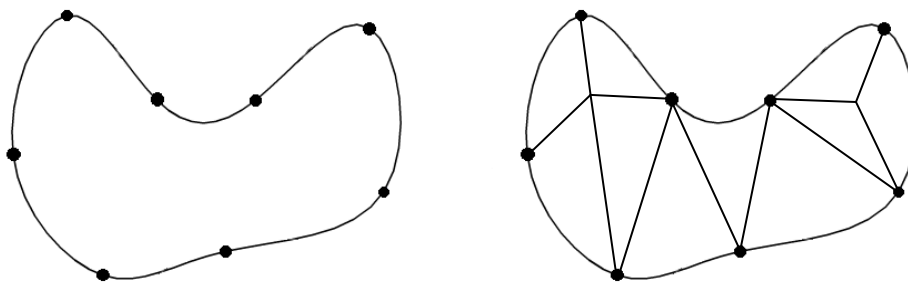


Figure 7: a) NURBS boundary with knots b) meshing with Bézier triangles.

If instead of a planar domain we have a NURBS surface, the Bézier triangles from the NURBS representation can be obtained by a process known as Bézier extraction (Hennig et al., 2016), (de Borst and Chen, 2018), (Goldman and Filip, 1987). The important point is that all the information regarding the geometry is contained in each Bézier triangle and can be used for adaptive refinement without any query to the geometric database.

3 A RATIONAL BÉZIER FINITE ELEMENT

The main idea of this work is to separate the interpolation for variables and geometry, then a conventional finite element interpolation can be used for variables and a Bézier interpolation for the geometry. A triangular finite element for stress analysis with a cubic Bézier geometry and a linear interpolation for displacements is developed to exemplify the procedure.

Assuming that the components of displacement u, v in the directions x, y are approximated by linear interpolation functions as

$$u(\xi_1, \xi_2, \xi_3) = \sum_{i=1}^3 \xi_i u_i = \mathbf{N}^T \mathbf{u} \quad (15)$$

$$v(\xi_1, \xi_2, \xi_3) = \sum_{i=1}^3 \xi_i v_i = \mathbf{N}^T \mathbf{v}$$

Where u_i, v_i are the displacement nodal values of the linear interpolation

$$\mathbf{u} = \{u_1 \quad u_2 \quad u_3\}^T \quad (16)$$

$$\mathbf{v} = \{v_1 \quad v_2 \quad v_3\}^T$$

And \mathbf{N} is the vector of linear shape functions

$$\mathbf{N} = \{\xi_1 \quad \xi_2 \quad \xi_3\}^T \quad (17)$$

The principle of the virtual displacements for a deformable finite element can be stated as

$$\delta W = \int_A \delta \boldsymbol{\varepsilon}^T \boldsymbol{\sigma} h dA - \delta W_{ext} = 0 \quad (18)$$

Where h is the thickness, δW_{ext} is the virtual work of external loads, $\boldsymbol{\sigma}$ is the stress field

$$\boldsymbol{\sigma} = \{\sigma_{xx} \quad \sigma_{yy} \quad \sigma_{xy}\}^T \quad (19)$$

And $\boldsymbol{\varepsilon}$ is the strain field

$$\boldsymbol{\varepsilon} = \{\varepsilon_{xx} \quad \varepsilon_{yy} \quad \gamma_{xy}\}^T \quad (20)$$

Where the strain components are

$$\varepsilon_{xx} = \frac{\partial u}{\partial x} \quad \varepsilon_{yy} = \frac{\partial v}{\partial y} \quad \gamma_{xy} = \frac{\partial u}{\partial y} + \frac{\partial v}{\partial x} \quad (21)$$

Replacing the finite element approximations, we have

$$\boldsymbol{\varepsilon} = \mathbf{B}\mathbf{d} \quad (22)$$

Where \mathbf{d} is the vector of nodal displacements of the mesh

$$\mathbf{d} = \{u_1 \quad v_1 \quad u_2 \quad v_2 \quad u_3 \quad v_3\}^T \quad (23)$$

And the gradient matrix \mathbf{B} is

$$\mathbf{B} = [\mathbf{B}_1 \quad \mathbf{B}_2 \quad \mathbf{B}_3] \quad (24)$$

The nodal matrices \mathbf{B}_i for linear shape functions are

$$\mathbf{B}_i = \begin{bmatrix} \frac{\partial N_i}{\partial x} & 0 \\ 0 & \frac{\partial N_i}{\partial y} \\ \frac{\partial N_i}{\partial y} & \frac{\partial N_i}{\partial x} \end{bmatrix} = \begin{bmatrix} \frac{\partial \xi_i}{\partial x} & 0 \\ 0 & \frac{\partial \xi_i}{\partial y} \\ \frac{\partial \xi_i}{\partial y} & \frac{\partial \xi_i}{\partial x} \end{bmatrix} \quad (25)$$

The stress vector $\boldsymbol{\sigma}$ is related to the strain vector $\boldsymbol{\varepsilon}$ by the constitutive matrix \mathbf{C} as

$$\boldsymbol{\sigma} = \mathbf{C}\boldsymbol{\varepsilon} = \mathbf{C}\mathbf{B}\mathbf{d} \quad (26)$$

For any variation $\delta\mathbf{d}$ of the nodal displacements, the variations of the strain field and the external virtual work are

$$\delta\boldsymbol{\varepsilon} = \mathbf{B}\delta\mathbf{d}, \quad \delta W_{ext} = \delta\mathbf{d}^T \mathbf{f}_{ext} \quad (27)$$

Where \mathbf{f}_{ext} is the vector of external loads. Then the virtual work is

$$\delta W = \delta\mathbf{d}^T \left(\int_A \mathbf{B}^T \boldsymbol{\sigma} h dA - \mathbf{f}_{ext} \right) = 0 \quad (28)$$

Since this equation must be valid for any variation $\delta\mathbf{d}$ then we must have

$$\mathbf{f}_{int} = \int_A \mathbf{B}^T \boldsymbol{\sigma} h dA = \mathbf{K}\mathbf{d} = \mathbf{f}_{ext} \quad (29)$$

Where \mathbf{f}_{int} is the vector of internal forces and \mathbf{K} is the stiffness matrix that can be written as

$$\mathbf{K} = \int_A \mathbf{B}^T \mathbf{C} \mathbf{B} h dA \quad (30)$$

This integral must be computed over the curved triangle, but it is convenient to do a coordinate transformation to integrate in area coordinates.

3.1 Transformation of coordinates

The differential area element dA is given by

$$dA = J d\xi_1 d\xi_2 d\xi_3 \quad (31)$$

Where for a general Bézier triangle of order n with $(n+1)(n+2)/2$ control points \mathbf{P}_{ijk} with coordinates x_{ijk} , y_{ijk} the jacobian J of the transformation is defined as (Felippa, 2015)

$$J = \frac{1}{2} \det \begin{bmatrix} 1 & 1 & 1 \\ \sum_{i+j+k=3} \frac{\partial M_{ijk}^n}{\partial \xi_1} x_{ijk} & \sum_{i+j+k=3} \frac{\partial M_{ijk}^n}{\partial \xi_2} x_{ijk} & \sum_{i+j+k=3} \frac{\partial M_{ijk}^n}{\partial \xi_3} x_{ijk} \\ \sum_{i+j+k=3} \frac{\partial M_{ijk}^n}{\partial \xi_1} y_{ijk} & \sum_{i+j+k=3} \frac{\partial M_{ijk}^n}{\partial \xi_2} y_{ijk} & \sum_{i+j+k=3} \frac{\partial M_{ijk}^n}{\partial \xi_3} y_{ijk} \end{bmatrix} \quad (32)$$

The derivatives of the shape functions M_{ijk}^3 are

$$\frac{\partial M_{ijk}^n(\xi_1, \xi_2, \xi_3)}{\partial \xi_p} = \frac{(\partial B_{ijk}^n / \partial \xi_p W_n - B_{ijk}^n \partial W_n / \partial \xi_p) w_{ijk}}{(W_n)^2} \quad (33)$$

Where

$$W_n(\xi_1, \xi_2, \xi_3) = \sum_{i+j+k=n} B_{ijk}^n(\xi_1, \xi_2, \xi_3) w_{ijk} \quad (34)$$

And the derivative of the Bernstein functions with respect to ξ_1 is

$$\frac{\partial B_{ijk}^n}{\partial \xi_1} = \binom{n}{i, j, k} i \xi_1^{i-1} \xi_2^j \xi_3^k \quad (35)$$

Analogously with the derivatives with respect to ξ_2, ξ_3 .

For the gradient matrix (45) the derivatives $\partial \xi_p / \partial x$ and $\partial \xi_p / \partial y$ can be calculated as (Felippa, 2015)

$$\begin{aligned} \frac{\partial \xi_p}{\partial x} &= \frac{1}{2J} \sum_{i+j+k=3} \left(\frac{\partial M_{ijk}^n}{\partial \xi_q} - \frac{\partial M_{ijk}^n}{\partial \xi_r} \right) y_{ijk} \\ \frac{\partial \xi_p}{\partial y} &= \frac{1}{2J} \sum_{i+j+k=3} \left(\frac{\partial M_{ijk}^n}{\partial \xi_r} - \frac{\partial M_{ijk}^n}{\partial \xi_q} \right) x_{ijk} \end{aligned} \quad (36)$$

Where cyclic permutation of indices p, q, r must be applied.

3.2 Integration of the stiffness matrix in area coordinates

After replacing the gradient matrix, the integrand of the stiffness matrix becomes a function of area coordinates ξ_1, ξ_2, ξ_3 then a coordinate transformation must be applied to obtain the stiffness matrix as

$$K = \int_A \mathbf{B}^T \mathbf{C} \mathbf{B} h J d\xi_1 d\xi_2 d\xi_3 \quad (37)$$

Note that the elements of the matrix \mathbf{B} and the jacobian J are rational functions of the area coordinates so direct analytical integration is complicated. The usual procedure is to apply numerical integration, but a simplified integration procedure will be employed.

4 A SIMPLIFIED INTEGRATION OF THE STIFFNESS MATRIX

The idea is to replace the gradient matrix \mathbf{B} by an approximated matrix $\bar{\mathbf{B}}$, this procedure is known as the B-bar approach (Simo and Hughes, 1986). Matrix \mathbf{B} is approximated by its Taylor series about the element centroid ($\zeta_1 = \zeta_2 = \zeta_3 = 1/3$) (Liu et al., 1985)

$$\mathbf{B} = \mathbf{B}|_c + \frac{\partial \mathbf{B}}{\partial \zeta_1} \left(\zeta_1 - \frac{1}{3} \right) + \frac{\partial \mathbf{B}}{\partial \zeta_2} \left(\zeta_2 - \frac{1}{3} \right) + \frac{\partial \mathbf{B}}{\partial \zeta_3} \left(\zeta_3 - \frac{1}{3} \right) + \dots \quad (38)$$

To ensure convergence, terms up to the same order of the undistorted element must be retained (Liu et al., 1994). Since a linear displacement field has been adopted, a constant approximated gradient matrix must be employed.

$$\bar{\mathbf{B}} = \mathbf{B}|_c = \mathbf{B}\left(\frac{1}{3}, \frac{1}{3}, \frac{1}{3}\right) \quad (39)$$

A constant jacobian $J_c = J\left(\frac{1}{3}, \frac{1}{3}, \frac{1}{3}\right)$ is also assumed. Then, the stiffness matrix is

$$\mathbf{K} \approx \int_A \bar{\mathbf{B}}^T \mathbf{C} \bar{\mathbf{B}} h J_c d\zeta_1 d\zeta_2 d\zeta_3 = \bar{\mathbf{B}}^T \mathbf{C} \bar{\mathbf{B}} h A \quad (40)$$

Where A is the area of the reference triangle (Cook et al., 2001)

$$A = \frac{1}{2} [(x_{030} - x_{300})(y_{003} - y_{300}) - (x_{003} - x_{300})(y_{030} - y_{300})] \quad (41)$$

The procedure can be applied with polynomials of high order for the displacement field, but, as a rule, the Taylor expansion of matrix \mathbf{B} must be always truncated to the same order of an undistorted element to guarantee convergence to the exact solution when the size of element tends to zero.

The patch test is passed for undistorted triangles of straight sides, so convergence is achieved in the limit when the refined elements become undistorted. Additionally, the procedure gives no spurious modes with zero energy since it converges to the classical linear finite element triangle which is stable.

5 NUMERICAL EXPERIMENTS

A square plate with a central hole under uniform tensile traction q on the right side is analyzed. The parameters for this problem are: length $l = 4$, radius $r = 1$, $q = 1$ and the material properties are $E = 1000$, $\nu = 0.3$ and unit thickness. All parameters are in compatible units. Due to symmetry, only a quarter of the plate is analyzed, and plane stress condition is assumed. An initial mesh of five elements is successively refined (Figure 8).

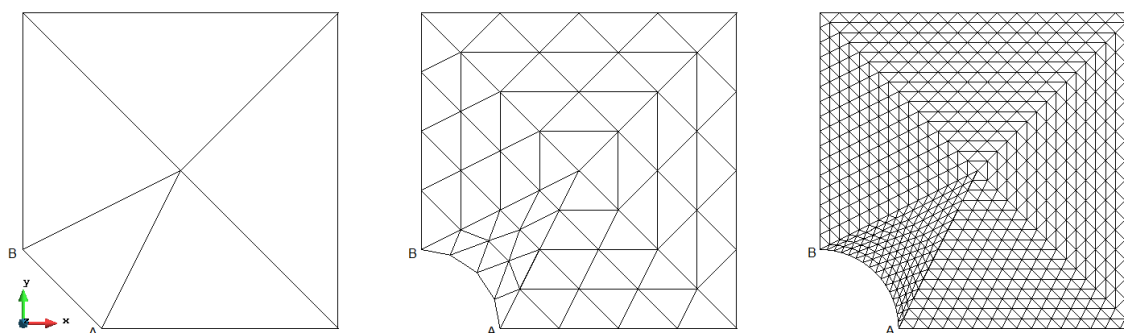


Figure 8: Some of the meshes employed obtained by uniform refinement.

The results of the analysis are shown in Table 1. The value of the horizontal displacement u corresponds to point A and the maximum horizontal stress σ_x corresponds to point B (see Figure 8).

nodes	elements	linear triangle		Beziér triangle	
		u at A	σ_x max	u at A	σ_x max
6	5	0.001817	1.207603	0.002212	1.292250
16	20	0.002619	1.703254	0.002810	1.829486
51	80	0.003217	2.347071	0.003282	2.404125
181	320	0.003501	2.898322	0.003518	2.915928
681	1280	0.003592	3.246309	0.003596	3.252498
2641	5120	0.003615	3.426818	0.003616	3.430446
10401	20480	0.003621	3.511488	0.003621	3.512952

Table 1: Plate with a hole under uniform traction

The results for the maximum stress σ_x converge to the exact value 3.6 (Timoshenko and Goodier, 1951) for both elements. As expected similar results are obtained since in this problem the influence of the geometry disappears for the finer meshes. The increase in total CPU time for the Beziér triangle (not shown in Table 1) is minimal since the stiffness matrices are of equal sizes for both elements.

6 CONCLUSIONS

A finite element formulation for stress analysis on planar domains with curved boundaries described by NURBS curves has been presented. Different interpolations are adopted for geometry and displacements. Rational Bézier polynomials on curved triangles are used for geometry description which can interpolate NURBS boundaries. Usual polynomials are used for the displacement field, in fact any type of proved convergent formulation on an undistorted triangular element can be employed, including mixed and hybrid formulations. The present procedure does not require numerical integration since the integrands are always polynomials that can be integrated exactly. The complexity of the formulation increases with the order of the Bézier interpolation and an intensive numerical comparison is necessary to decide if a simple formulation with straight sided triangles, but retaining the Bézier information for adaptive refinement, can be competitive.

REFERENCES

- Adam, C., Bouabdallah, S., Zarroug, M., Maitournam, H. Improved numerical integration for locking treatment in isogeometric structural elements. Part II: Plates and shells. *Computer Methods in Applied Mechanics and Engineering*, Isogeometric Analysis Special Issue 284, 106–137, 2015a.
- Adam, C., Hughes, T.J.R., Bouabdallah, S., Zarroug, M., Maitournam, H. Selective and reduced numerical integrations for NURBS-based isogeometric analysis. *Computer Methods in Applied Mechanics and Engineering*, Isogeometric Analysis Special Issue 284, 732–761, 2015b.
- Cook, R.D., Malkus, D.S., Michael E. Plesha, Witt, R.J., *Concepts and applications of finite element analysis*, 4th ed. Wiley, 2001.
- Cottrell, J.A., Hughes, T.J.R., Bazilevs, Y., *Isogeometric Analysis: Toward Integration of CAD and FEA*. John Wiley & Sons, 2009.
- Cottrell, J.A., Hughes, T.J.R., Reali, A. Studies of refinement and continuity in isogeometric structural analysis. *Computer Methods in Applied Mechanics and Engineering*, 196, 4160–4183, 2007.

- de Borst, R., Chen, L. The role of Bézier extraction in adaptive isogeometric analysis: Local refinement and hierarchical refinement. *International Journal for Numerical Methods in Engineering*, 113, 999–1019, 2018.
- Engvall, L., Evans, J.A. Isogeometric triangular Bernstein–Bézier discretizations: Automatic mesh generation and geometrically exact finite element analysis. *Computer Methods in Applied Mechanics and Engineering*, 304, 378–407, 2016.
- Fahrendorf, F., De Lorenzis, L., Gomez, H. Reduced integration at superconvergent points in isogeometric analysis. *Computer Methods in Applied Mechanics and Engineering*, 328, 390–410, 2018.
- Farin, G. *Curves and Surfaces for CAGD: A Practical Guide*. Morgan Kaufmann, 2002.
- Farin, G. Triangular Bernstein–Bézier patches. *Computer Aided Geometric Design*, 3, 83–127, 1986.
- Felippa, C.A. *Introduction to Finite Elements: Implementation of Iso-P Triangular Elements*. Course Notes. <https://www.colorado.edu/engineering/Aerospace/CAS/courses.d/IFEM.d/>, 2015.
- George, P.L., Borouchaki, H. Construction of tetrahedral meshes of degree two. *International Journal for Numerical Methods in Engineering*, 90, 1156–1182, 2012.
- Godoy, L.A. *Thin-Walled Structures with Structural Imperfections*. Elsevier, 1996.
- Goldman, R.N., Filip, D.J. Conversion from Bézier rectangles to Bézier triangles. *Computer-Aided Design*, 19, 25–27, 1987.
- Hennig, P., Müller, S., Kästner, M. Bézier extraction and adaptive refinement of truncated hierarchical NURBS. *Computer Methods in Applied Mechanics and Engineering*, 305, 316–339, 2016.
- Hughes, T.J.R., Cottrell, J.A., Bazilevs, Y. Isogeometric analysis: CAD, finite elements, NURBS, exact geometry and mesh refinement. *Computer Methods in Applied Mechanics and Engineering*, 194, 4135–4195, 2005.
- Jaxon, N., Qian, X. Isogeometric analysis on triangulations. *Computer-Aided Design*, 2013 SIAM Conference on Geometric and Physical Modeling 46, 45–57, 2014.
- Jouglaard, C.E., Sarpero, C.J., Ferrari, F.J. Un Elemento Finito Triangular NURBS Simplificado para Análisis de Tensiones. *Mecánica Computacional*, 31, 1045–1064, 2012.
- Liu, W.K., Hu, Y.-K., Belytschko, T. Multiple quadrature underintegrated finite elements. *International Journal for Numerical Methods in Engineering*, 37, 3263–3289, 1994.
- Liu, W.K., Ong, J.S.-J., Uras, R.A. Finite element stabilization matrices—a unification approach. *Computer Methods in Applied Mechanics and Engineering*, 53, 13–46, 1985.
- Marussig, B., Hughes, T.J.R. A Review of Trimming in Isogeometric Analysis: Challenges, Data Exchange and Simulation Aspects. *Archives of Computational Methods in Engineering*, 1–69, 2017.
- Piegl, L., Tiller, W. *The NURBS Book*. Springer Science & Business Media, 1997.
- Sevilla, R., Fernández-Méndez, S., Huerta, A. NURBS-enhanced finite element method (NEFEM). *International Journal for Numerical Methods in Engineering*, 76, 56–83, 2008.
- Simo, J.C., Hughes, T.J.R. On the Variational Foundations of Assumed Strain Methods. *ASME Journal of Applied Mechanics*. 53, 51–54, 1986.
- Godoy, L.A. *Thin-Walled Structures with Structural Imperfections*. Elsevier, 1996.
- Timoshenko S., and Goodier J. N. *Theory of Elasticity*. McGraw-Hill book Company, 1951.
- Xia, S., Qian, X. Isogeometric analysis with Bézier tetrahedra. *Archives of Computational Methods in Engineering*, Special Issue on Isogeometric Analysis: Progress and Challenges 316, 782–816, 2017.
- Zienkiewicz, O.C., Taylor, R.L., Zhu, J.Z. *The Finite Element Method: Its Basis and Fundamentals*, 7th ed. Elsevier Butterworth-Heinemann, 2013.